Structure in the parameter dependence of order and chaos for the quadratic map

1997 J. Phys. A: Math. Gen. 30 7067

(http://iopscience.iop.org/0305-4470/30/20/012)

J. Phys. A: Math. Gen. **30** (1997) 7067–7076. Printed in the UK PII: S0305-4470(97)77599-1

Structure in the parameter dependence of order and chaos for the quadratic map

Brian R Hunt† and Edward Ott‡

† Institute for Physical Science and Technology, University of Maryland, College Park, MD 20742, USA

‡ Departments of Electrical Engineering and of Physics, Institute for Plasma Research and Institute for Systems Research, University of Maryland, College Park, MD 20742, USA

Received 4 September 1996, in final form 23 June 1997

Abstract. Many dynamical systems are thought to exhibit windows of attracting periodic behaviour for arbitrarily small perturbations from parameter values yielding chaotic attractors. This structural instability of chaos is particularly well documented and understood for the case of the one-dimensional quadratic map. In this paper we attempt to numerically characterize the global parameter-space structure of the dense set of periodic 'windows' occurring in the chaotic regime of the quadratic map. In particular, we use scaling techniques to extract information on the probability distribution of window parameter widths as a function of period and location of the window in parameter space. We also use this information to obtain the uncertainty exponent which is a quantity that globally characterizes the ability to identify chaos in the presence of small parameter uncertainties.

1. Introduction

The quadratic map may be expressed in the form

$$x_{n+1} = x_n^2 - C. \tag{1}$$

Because of its relative simplicity and ease of numerical study, this map has proven to be an invaluable model for revealing various kinds of characteristic nonlinear dynamical behaviour (e.g. period-doubling cascades, pairwise merging of chaotic bands, intermittency, crises, etc). (We choose to write the quadratic map in the form (1) because, for $C = 0$, the period one attractor is at $x = 0$ and is superstable (i.e. $x_{n+1} = x_n$ and $\mathrm{d}x_{n+1}/\mathrm{d}x_n = 0$ at $x_n = C = 0$). This will prove convenient in a later discussion.) There is a unique bounded attractor for (1) for

$$2 \geqslant C \geqslant -\tfrac{1}{4}.$$

Jacobson[1] proved that the set of C values for which the attractor of (1) is chaotic has positive Lebesgue measure. More recently, Graczyk and Świątek[2] proved that the set of C values corresponding to attracting periodic orbits is dense in the set of chaotic C values. These periodic orbits occur in 'windows' in parameter space. A period p window begins as C increases through a lower critical value at which a period p tangent bifurcation creates a stable (attracting) period p orbit and an unstable (repelling) period p orbit. As C increases, the attracting period p orbit goes through a period-doubling cascade to chaos, and the attractor apparently widens into p narrow chaotic bands through which the orbit consecutively cycles. The window ends as C increases through an upper critical value at which the p orbit points of the unstable period p orbit, created at the original tangent bifurcation, first touch the edges of the p chaotic bands of the chaotic attractor (a *crisis*). The largest and most familiar example of a window is the famous period-three window of (1), which occupies the interval $1.75 \leqslant C \leqslant 1.79\ldots$. For large p, the number N_p of windows with period p in the entire range $2 \geqslant C \geqslant -\frac{1}{4}$ is large,

$$N_p \cong (2^p - 2)/(2p) \tag{2}$$

and this approximate expression becomes exact if p is prime (e.g. see [3]).

In this paper we attempt to characterize statistically the global parameter-space structure of the dense set of windows in the chaotic regime of (1). In particular, we seek information on the large p behaviour of the probability distribution of window widths in C as a function of the period and the location of the window in parameter space†. We also use this information to obtain the uncertainty exponent (defined in section 2.2). In addressing these questions our approach will be to combine numerical analysis with scaling techniques. While it is not clear from our numerical results whether or not the scaling hypothesis we use is true exactly, it will be shown that our hypothesis holds at least approximately and that it provides a very useful way of organizing the data.

2. Background

2.1. The width of a window

We may regard the attractor within a window as always residing in p narrow intervals in x. Throughout the entire range of the parameter C within a given period p window, the attracting orbit, whether it is periodic or chaotic, consecutively cycles through these p narrow x intervals. As shown below, these intervals tend to become narrower, and the window parameter width becomes smaller, as p increases. Of the p intervals in x, one straddles the critical point (i.e. the maximum of the map function, $x = 0$ for (1)), while the other $(p - 1)$ intervals are typically [5] located away from the critical point.

We now use the above discussion to obtain an estimate [5] of the window parameter width ΔC_p. We consider the pth iterate of the map $x_{n+p} = F^{(p)}(x_n, C)$ for C in a period p window and x_n in the central x-interval that straddles the critical point. We expand the equation $x_{n+p} = F^{(p)}(x_n, C)$, for x_n and x_{n+p} small (they are in the narrow interval about $x = 0$) and C near its value C_{ss} at superstability of the period p attracting orbit. Because of the narrowness of the $(p - 1)$ intervals that are away from the critical point, we can use a linear approximation to the map in those intervals; the full quadratic (1) must be retained for the central interval. One thus obtains [5]

$$x_{n+p} \cong \Lambda_p[x_n^2 - (C - C_{ss})] \tag{3}$$

where $\Lambda_p = \lambda_1\lambda_2\ldots\lambda_{p-1}$ is the product of the map slopes, $\lambda_i = 2x_{n+i}$, in the $(p - 1)$ noncentral intervals‡. Since we are in the region of C values where chaos is possible, the λ_i are typically of magnitude larger than one, and, consequently, $|\Lambda_p|$ is large for large p. While Λ_p varies with x_n and with C through the parameter range of the window, this

† A different approach is used in Post and Capel [4] where a precise estimate of the width of a window in terms of the location (in both parameter and phase space) of the superstable orbit within the window is obtained, and this estimate is used to study the scaling of widths of particular families of windows.

‡ More accurately, equation (3) should read $x_{n+1} \cong \Lambda_p[x_n^2 - \beta(C - C_{sc})]$, where β is of order 1 and is given by $\beta = 1 + \lambda_1^{-1} + (\lambda_1\lambda_2)^{-1} + \cdots + (\lambda_1\lambda_2\ldots\lambda_{p-1})^{-1}$. Since we will be dealing with the logarithm of the window width for small window widths, the factor β of order 1 is not important and for simplicity we set it to 1.

variation is small for narrow windows. Thus we have treated Λ_p as if it were a constant in the window. For definiteness we, henceforth, take Λ_p as the value at the superstable period p orbit in the window.

Introducing $\tilde{x} = \Lambda_p x$ and $\tilde{C}_p = \Lambda_p^2(C - C_{ss})$, equation (3) becomes

$$\tilde{x}_{n+p} \cong \tilde{x}_n^2 - \tilde{C}_p$$

which is identical in form to equation (1). Thus one expects (and numerically observes) that, as C is increased, the bifurcation diagram restricted to the central band of a window, when magnified, approximately replicates the bifurcation diagram of (1) in the entire interval $2 \geqslant C \geqslant -\frac{1}{4}$. (The period-one attractor of (1) is born by a tangent bifurcation as C increases through $-\frac{1}{4}$, and the final single-band chaotic attractor of (1) is destroyed by a crisis as C increases through 2.) Furthermore, unnormalizing, we find that the window width is

$$\Delta C_p \cong (\tfrac{9}{4})\Lambda_p^{-2} \tag{4}$$

while the x width of the central interval scales as Λ_p^{-1}. Since Λ_p becomes large for large p, these widths become small. It is argued in [5] that the above analysis is good save for an exponentially (in p) small fraction of exceptional windows, and that, for the nonexceptional windows, results, such as (4), are true asymptotically for large p.

Since each window replicates the bifurcation diagram of the map (1) over the full range $2 \geqslant C \geqslant -\frac{1}{4}$, there are an infinite number of windows of period divisible by p in each period p window. We refer to those windows that do not appear within another window as *primary* windows. The fraction of the N_p windows of period p (see equation (2)) that are not primary may be shown to approach zero as $p \to +\infty$ (this fraction is trivially zero for p a prime number).

2.2. *Uncertainty exponent*

The uncertainty exponent (originally introduced [6] to describe fractal basin boundaries) can be applied to the set S_c of C values for which equation (1) yields a chaotic attractor. Say we randomly choose a value of C in the set S_c (where the random choice is with respect to the Lebesgue measure of S_c). Now choose a second value of C by perturbing the first value by the addition of a small randomly chosen number δ, where δ is chosen at random with uniform probability density in the interval $-\epsilon \leqslant \delta \leqslant \epsilon$. Let $\bar{P}(\epsilon)$ be the probability that the perturbed value yields a periodic (rather than a chaotic) attractor. The uncertainty exponent is then defined as

$$\alpha = \lim_{\epsilon \to 0} \frac{\log \bar{P}(\epsilon)}{\log \epsilon}. \tag{5}$$

In more concrete terms, $\bar{P}(\epsilon)$ is the probability of making an error when one predicts that the orbit is chaotic given a C value with measurement uncertainty ϵ, and α gives the ϵ scaling of this error probability, $\bar{P}(\epsilon) \sim \epsilon^\alpha$.

Another, slightly different, way of defining the uncertainty exponent is as follows. Let $S_c(\epsilon)$ be the set created by fattening S_c by the amount ϵ. By this we mean that we take the original set plus all points within a distance ϵ from S_c. The other uncertainty exponent definition is then given by

$$\alpha = \lim_{\epsilon \to 0} \frac{\log V[\bar{S}_c(\epsilon)]}{\log \epsilon} \tag{6}$$

where V denotes Lebesgue measure and $\bar{S}_c(\epsilon) = S_c(\epsilon) - S_c$ is what remains if the original set S_c is deleted from the fattened set $S_c(\epsilon)$.

The connection between (5) and (6) can be understood as follows. Consider C_1 and C_2 chosen at random with respect to Lebesgue measure, subject to the condition that $|C_1 - C_2| \leqslant \epsilon$. Then $\bar{P}(\epsilon)$ represents the conditional probability that $C_2 \in \bar{S}_c(\epsilon)$ given that $C_1 \in S_c$. Let $\tilde{P}(\epsilon)$ represent the conditional probability that $C_1 \in S_c$ given that $C_2 \in \bar{S}_c(\epsilon)$. Then

$$\tilde{P}(\epsilon) = \bar{P}(\epsilon)\frac{V[S_c]}{V[\bar{S}_c(\epsilon)]}.$$

It follows that the limits in (5) and (6) are the same provided that $\tilde{P}(\epsilon)$ approaches a positive constant as $\epsilon \to 0$. Thinking of S_c as the complement of the periodic windows in parameter space, every $C_2 \in \bar{S}_c(\epsilon)$ lies within ϵ of the boundary of the window that contains it. Considering all such C_2 within a given window, and all C_1 within ϵ of C_2, the probability that C_1 is outside the given window is at least $\frac{1}{4}$. It is possible that C_1 lies in another window, but both numerical evidence and the fact that S_c has positive Lebesgue measure suggest that for small ϵ, if C_1 is outside a window but within ϵ of its boundary, then the probability that $C_1 \in S_c$ is high. It then follows that $\tilde{P}(\epsilon)$ stays close to or above $\frac{1}{4}$ as $\epsilon \to 0$, and that (5) and (6) are equivalent for S_c.

In [7] Farmer found a scaling by calculating the C ranges of a large number of primary windows. His scaling was obtained by a procedure that essentially approximates α as defined by (6). He obtains $\alpha \cong 0.45 \pm 0.04$.

In [8] α was numerically evaluated from the definition (5) by perturbing C values in S_c by $\pm\epsilon$. Whether the resulting orbits are chaotic or not was determined from the sign of the numerically calculated Lyapunov exponent. The fraction of orbits in S_c yielding a nonchaotic perturbed orbit is then calculated using a large number of randomly chosen initial conditions in S_c. The scaling of this fraction with decreasing ϵ then gives the uncertainty exponent. The resulting estimate of α for the quadratic map [8] was $\alpha \cong 0.41$.

3. Heuristic analysis

Based on Λ_p we can define an effective *window Lyapunov exponent* for each window,

$$\tilde{h}_p = \frac{1}{p-1}\log|\Lambda_p| \tag{7}$$

where we evaluate Λ_p at superstability. From equation (4) knowledge of the statistics of $\tilde{h}_p$ is equivalent to knowledge of the statistics of the window widths.

The statistics of finite-time Lyapunov exponents have been studied for chaotic maps with *fixed* parameter values [9]. In this case, one imagines choosing an initial condition x_1 at random with respect to the natural measure on the chaotic attractor of the (fixed) map. Using this initial condition one next calculates the finite time Lyapunov exponent $h_n = n^{-1}\log|F'(x_1)F'(x_2)\ldots F'(x_n)|$, where $x_1, x_2, \ldots, x_n$ are the first n points of the chaotic orbit from the randomly chosen x_1. It is then argued that the probability distribution function of the random variable h_n is [9]

$$P_n(h) \cong \sqrt{\frac{nH''(\bar{h})}{2\pi}}\exp[-nH(h)] \tag{8}$$

for large n, where $H(\bar{h}) = 0$ and the function $H(h) \geqslant 0$ is concave up; in particular, $H''(\bar{h}) > 0$ and $H(h)$ increases for increasing $|h - \bar{h}|$. The utility of equation (8) is that it expresses the function $P_n(h)$, which depends on the *two* variables n and h, in terms of a function of a *single* variable, $H(h)$. Note that in the limit $n \to +\infty$, equation (8) yields

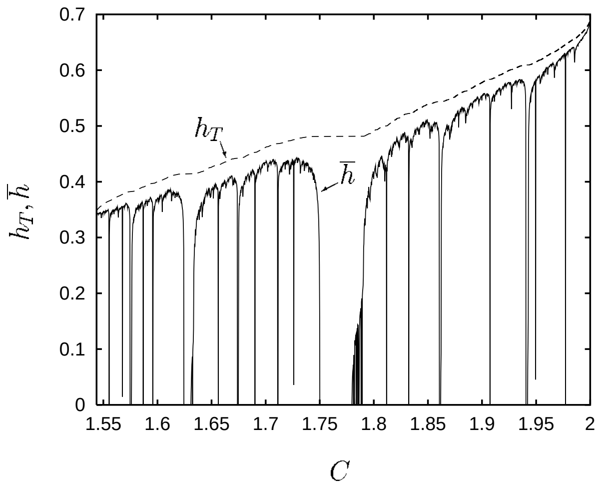

Figure 1. Topological entropy h_T and Lyapunov exponent $\bar{h}$ versus the parameter C. The Lyapunov exponent was computed for 2000 evenly spaced parameter values using 10^8 iterations for each value; only positive exponents are shown.

the Dirac distribution $\delta(h - \bar{h})$ so that with probability 1 the limit as $n \to +\infty$ of h_n is $\bar{h}$. Thus the quantity $\bar{h}$ is what is conventionally called *the* Lyapunov exponent. Equation (8) has been tested numerically with good results for a number of chaotic processes.

We would like to obtain something similar to equation (8) for the window Lyapunov exponents given by equation (7). The reason we cannot apply equation (8) directly is that it is obtained for a fixed map and a randomly chosen initial condition. In contrast, we take our initial condition at $x_1 = 0$ for C at its superstable point in a period p window. What we desire is to choose one of the $N_p \gg 1$ windows of period p at random and to hypothesize a probability distribution like equation (8) for $\tilde{h}_p$, the argument being that, for large p, the periodic orbit paths with different C values are like chaotic orbits from different initial conditions except that at the end the orbit happens to return to $x = 0$. This, however, does not yet make sense as can be seen from figure 1, which shows the Lyapunov exponent $\bar{h}$ and topological entropy h_T of (1) versus C. The Lyapunov exponent $\bar{h}$ varies erratically with C as implied by the denseness of attracting periodic orbits ($\bar{h} < 0$) in the set of C values yielding chaos ($\bar{h} > 0$). Note, however, that the topological entropy, which gives a more global measure of chaos, varies continuously with C. Thus, from the h_T versus C plot, one expects inherent continuous C dependence in the distribution function of $\tilde{h}_p$ that is not included in (8). On the other hand, it would seem reasonable to take as a working assumption the supposition that $\tilde{h}_p$ for different period p windows fluctuates about a value proportional to h_T, where, of course, h_T has the C dependence in figure 1 (it may be shown that h_T is constant in a window). The reasoning here is that h_T provides a robust measure of the stretching, while $\tilde{h}_p$ characterizes the stretching in the window (with the central band deleted). This suggests introducing the normalization

$$\mathcal{H} = \tilde{h}_p / h_T. \tag{9}$$

Furthermore, since we deem the net stretching over a given time to be the relevant measure of time (rather than the number of iterates *per se*), we introduce the normalized period

$$m = p h_T. \tag{10}$$

In analogy to (8) we now hypothesize a scaling form for $P_m(\mathcal{H})$, the probability distribution of $\mathcal{H}$ at fixed large m,

$$P_m(\mathcal{H}) \cong \sqrt{\frac{G''(\bar{\mathcal{H}})}{2\pi m}} \exp[-mG(\mathcal{H})] \tag{11}$$

where the properties of $G(\mathcal{H})$ are the same as those stated for $H(h)$ in (8). Thus all the smooth C dependence of the variation of the character of the map is subsumed in the normalizations (9) and (10) and the C dependence of h_T. The worth of our hypothesis (11) is ultimately dependent on how well it models the data (see section 4).

We now explore the consequences of (11). In particular, we use (11) to obtain the uncertainty exponent α in terms of $G(\mathcal{H})$. A key point is that the number of windows with period p in the range $C \leqslant C'$ scales as

$$N_p(C \leqslant C') \sim \exp[ph_T(C')]. \tag{12}$$

(Note that for $C' = 2$, we have $h_T = \ln 2$, so that (12) gives $N_p \sim 2^p$ in agreement with (2).) Consider the set S_W of C values in windows. Since the Lebesgue measure of C values yielding periodic attractors within a window is larger than the Lebesgue measure of C values yielding chaos within the window, we estimate $V[\bar{S}_c(\epsilon)]$ in (6) as the Lebesgue measure of points in S_W that are within ϵ of a chaotic parameter value lying outside all windows. Making use of our scaling hypothesis (11), we have for C in the range $C \leqslant C'$

$$V[\bar{S}_c(\epsilon)] \sim \sum_{p=1}^{\infty} \mathrm{e}^{ph_T} \int_0^{\infty} P_{ph_T}(\mathcal{H}) \min(\epsilon, \mathrm{e}^{-2ph_T\mathcal{H}})\, \mathrm{d}\mathcal{H} \tag{13}$$

where $h_T = h_T(C')$, $\epsilon \ll 1$, and we have used (4), (7) and (9) to estimate the window width as

$$\Delta C_p \sim \exp(-2ph_T\mathcal{H}) \tag{14}$$

(the result for α will turn out to be independent of C'; i.e. independent of $h_T(C')$). The term $\min(\epsilon, \mathrm{e}^{-2ph_T\mathcal{H}})$ arises because a window of width $\Delta C_p < \epsilon$ is completely filled by the ϵ fattening (yielding a contribution to the Lebesgue measure of $\Delta C_p \sim \exp(-2h_T\mathcal{H})$), while a window of width $\Delta C_p > \epsilon$ is only filled by an amount of order ϵ (yielding a contribution of order ϵ to the Lebesgue measure).

Approximating the sum over p as an integral and introducing the scaling variable m, equation (13) becomes

$$V[\bar{S}_c(\epsilon)] \sim \int_0^{\infty} \mathrm{d}m \int_0^{\infty} \mathrm{d}\mathcal{H} \exp[m(1 - G(\mathcal{H}))] \min(\epsilon, \mathrm{e}^{-2m\mathcal{H}}). \tag{15}$$

Consider the dividing curve $\epsilon = \exp(-2m\mathcal{H})$ or $m\mathcal{H} = \frac{1}{2}\log(1/\epsilon)$ in the $(m, \mathcal{H})$ plane (see figure 2).

Below the dividing curve the integrand is

$$I_< = \epsilon \exp[m(1 - G(\mathcal{H}))] \tag{16}$$

while above the dividing curve the integrand is

$$I_> = \exp[m(1 - 2\mathcal{H} - G(\mathcal{H}))]. \tag{17}$$

For small ϵ the main contribution to the integral (15) comes from a small region of the $(m, \mathcal{H})$ plane in the vicinity of the maximum value of the integrand. Thus we need to determine the location of that maximum. Considering m as constant, $I_<$ is maximized with respect to $\mathcal{H}$ at the value of $\mathcal{H}$ for which $G(\mathcal{H})$ is minimum. This value is, by definition,

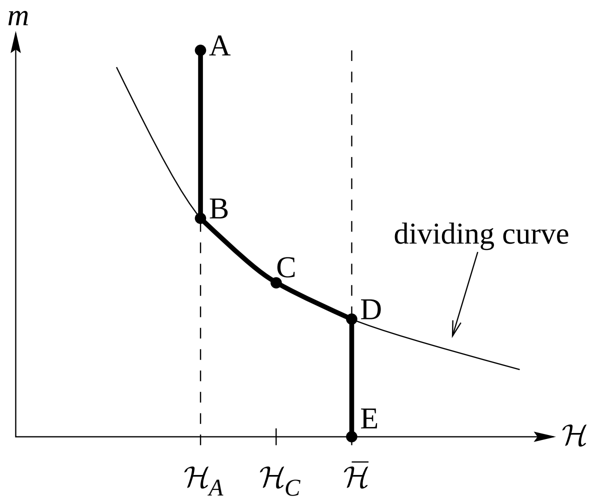

Figure 2. The dividing curve $m\mathcal{H} = \frac{1}{2}\log(1/\epsilon)$ for the integrand of (15) and the values of $\mathcal{H}$ discussed in locating the maximum of the integrand.

$\mathcal{H} = \bar{\mathcal{H}}$. Similarly, from the fact that $G(\mathcal{H})$ is a concave-up function of $\mathcal{H}$ we have that $I_>$ is maximized with respect to $\mathcal{H}$ with m fixed at $\mathcal{H} = \mathcal{H}_A$ where $\mathcal{H}_A$ is the solution of

$$G'(\mathcal{H}_A) = -2$$

and $G' \equiv \mathrm{d}G/\mathrm{d}\mathcal{H}$. Since G is concave up, $\mathcal{H}_A < \bar{\mathcal{H}}$; the situation is as depicted in figure 2. The function $I_<$ decreases monotonically as one moves horizontally away (either to the left or to the right) from the vertical line $\mathcal{H} = \bar{\mathcal{H}}$. The function $I_>$ likewise decreases monotonically as one moves horizontally away from the vertical line $\mathcal{H} = \mathcal{H}_A$. Thus for fixed m the integrand $\min(\Sigma_<, \Sigma_>)$ is maximized as a function of $\mathcal{H}$ on the curve ABDE highlighted in figure 2. On the segment DE, we have $I_< = \epsilon \mathrm{e}^m$, which increases monotonically with m. On the segment AB, we have $I_> = \exp[m(1 - 2\mathcal{H}_A - G(\mathcal{H}_A))]$, and we must assume $[1 - 2\mathcal{H}_A - G(\mathcal{H}_A)] < 0$ for convergence of the integral (15); thus on the segment AB, the quantity $I_>$ increases monotonically as m is decreased. The above discussed properties of $I_<$ and $I_>$ have the consequence that the maximum of the integrand lies on the dividing curve, $m\mathcal{H} = \log(1/\epsilon)^{1/2}$, somewhere between points B and D. We label this maximum point C in figure 2. On the dividing curve we express the integrand in terms of $\mathcal{H}$ by substituting $m = \mathcal{H}^{-1}\log(1/\epsilon)^{1/2}$ into either (16) or (17):

$$I = \epsilon^{\{1-[1-G(\mathcal{H})]/(2\mathcal{H})\}}.$$

The maximum of the above expression is obtained at $\mathcal{H} = \mathcal{H}_C$, where $\mathcal{H}_C$ is the solution of

$$1 - G(\mathcal{H}_C) + \mathcal{H}_C G'(\mathcal{H}_C) = 0. \tag{18}$$

Estimating $V[\bar{S}_c(\epsilon)]$ as $V[\bar{S}_c(\epsilon)] \sim \epsilon^\alpha$, we have

$$\alpha = 1 - \frac{1 - G(\mathcal{H}_C)}{2\mathcal{H}_C}. \tag{19}$$

An an example, we now consider the case where $G(\mathcal{H})$ is parabolic ($P_m(\mathcal{H})$ is Gaussian),

$$G(\mathcal{H}) = (\mathcal{H} - \bar{\mathcal{H}})^2/(2\delta^2\bar{\mathcal{H}}^2) \tag{20}$$

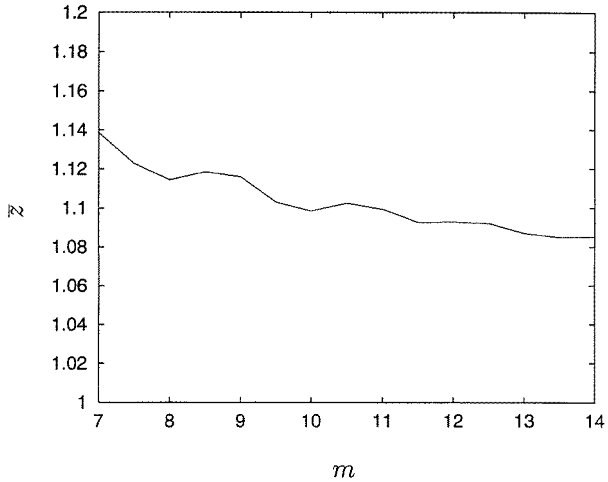

Figure 3. Mean $\bar{z}$ of normalized window widths versus m.

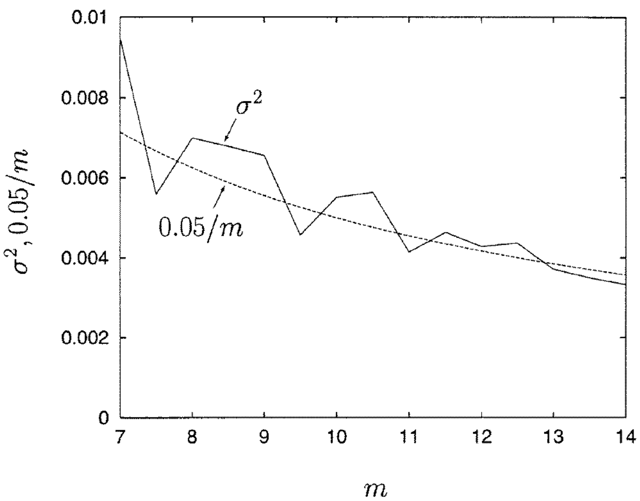

Figure 4. Variance σ^2 of normalized window widths versus m.

where δ denotes the relative standard deviation of fluctuations in $\mathcal{H}$ from the average value $\bar{\mathcal{H}}$. Equations (18)–(20) yield

$$\alpha = 1 - \frac{1}{\bar{\mathcal{H}}(1 + \sqrt{1 - 2\delta^2})}. \tag{21}$$

As a point of reference, if we neglect fluctuations ($\delta = 0$) and take h_p to be equal to h_T ($\bar{\mathcal{H}} = 1$), we obtain $\alpha = \frac{1}{2}$. This value is not too far off the numerically obtained values in [7] and [8]. To do better we now turn to numerical experiments.

4. Results of numerical experiments

In order to test the hypothesis (11), we performed an exhaustive search for windows of the quadratic map on the interval $1.5437\ldots \leqslant C \leqslant 2$ where the attractor is a single interval for C outside of the windows. We computed the window width ΔC_p and entropy h_T of windows of period p up to 40 and width at least 10^{-15}. There are approximately 2.75 million such windows. Recall that we have estimated in (14) that $\Delta C_p \cong \exp(-2ph_T\mathcal{H})$, and recall that $m = ph_T$. Rather than measure $\mathcal{H}$ directly for these windows, we computed the quantity

$$z = \frac{-\ln(\Delta C_p)}{2ph_T} = \frac{-\ln(\Delta C_p)}{2m} \tag{22}$$

which approximates $\mathcal{H}$. Thus we test whether z has the same type of probability distribution, for fixed m, as given by (11) for $\mathcal{H}$, namely that

$$P_m(z) \cong \sqrt{\frac{G''(\bar{z})}{2\pi m}} \exp[-mG(z)]. \tag{23}$$

In order to test the validity of (23) we divided the possible values of m into bins of width 0.5 and examined the statistics of z for windows in each bin $(m - 0.5, m]$. Figures 3 and 4 show respectively the computed mean $\bar{z}$ and variance σ^2 of z as a function of m for $7 \leqslant m \leqslant 14$.

The reasons for limiting our considerations to the range $7 \leqslant m \leqslant 14$ are as follows. For $m < 7$, the number of windows per bin drops below 100, and the computed statistics become unreliable. On the other hand, for $m > 14$ it is possible for the period $p = m/h_T$ of the window to exceed 40 because the entropy h_T can be as low as $(\ln 2)/2$ at the lower endpoint of the C interval we consider. Also for m near 14 the windows with width near 10^{-15} start to become significant in number; thus our limitations on the period and window width begin to bias the statistics as m increases past 14.

From figure 3 we see that as m increases, the mean value does seem to be approaching a value $1 < \bar{z} < 1.1$ which is independent of m, in accordance with our hypothesis. The predicted distribution also has the property that the variance σ^2 should vary inversely with m, and figure 4, though perhaps not conclusive, is consistent with the approximation $\sigma^2 \cong 0.05/m$.

In section 3 we estimated the uncertainty exponent α of the chaotic parameter set S_c in terms of the mean and standard deviation of the distribution for $\mathcal{H}$, assuming that G is quadratic. Approximating the statistics of $\mathcal{H}$ by those we measured for z, we plug the values $\bar{\mathcal{H}} = 1.05 \pm 0.05$ and $\delta^2 = 0.05 \pm 0.02$ into (21). The result is $\alpha = 0.51 \pm 0.03$, which is in line with the prediction that α is close to $\frac{1}{2}$.

Remark. Note that in [8] the set for which the uncertainty exponent is calculated is the set of C values yielding chaos, while in [7] it is the set of C values that yield chaos and are not in primary windows. (See the discussion of [7, 8] at the end of section 2) It is not clear whether or not one should expect the same α for these two sets. In our computation of α we have used the set of [7]; that is, we considered only chaotic behaviour that is not in a primary window. Since we also restricted consideration to the range of C between the merging point of the two-band chaotic attractor and the point of the final crisis ($C = 2$), our choice is equivalent to considering C values for which there is a one-piece chaotic attractor.

5. Discussion

For the quadratic map we have introduced the idea of a 'normalized period' $m = ph_T$ of a periodic window, where p is the period and h_T is the topological entropy of the dynamics in the window. Whereas windows with a given period p have tremendous variation in their widths, windows with similar values of m have much greater uniformity in width.

Specifically, (22) and (23) imply that for a given m, the natural logarithm of the window width has expected value near $-2m$ and standard deviation proportional to $\sqrt{m}$. Thus grouping the windows with common values of m provides a useful means for measuring the statistics of window widths. Further, the nature of these statistics allowed us to derive in section 3 the uncertainty exponent α of the chaotic parameter set in terms of quantities which are measurable from window data, and our results in section 4 agree with earlier measurements which indicate that α is in the vicinity of $\frac{1}{2}$.

Though all of our analysis has concerned the quadratic map, we expect that similar scaling results for window widths apply to other one-parameter families of one-dimensional maps with a single quadratic maximum.

Acknowledgments

This work was supported by the National Science Foundation (Divisions of Mathematical and Physical Sciences), the US Department of Energy (Mathematical, Information, and Computational Sciences Division, High Performance Computing and Communications Program), and by the Office of Naval Research. Numerical computations were performed using equipment provided by a grant from the W M Keck Foundation.

References

[1] Jacobson M V 1978 *Sov. Math. Dokl.* **19** 1452
[2] Graczyk J and Świątek G 1997 Hyperbolicity in the real quadratic family *Ann. Math.* to appear
[3] For example Ott E 1993 *Chaos in Dynamical Systems* (Cambridge: Cambridge University Press) p 29
[4] Post T and Capel H W 1991 *Physica* **178A** 62
[5] Yorke J A, Grebogi C, Ott E and Tedeschini-Lalli L 1985 *Phys. Rev. Lett.* **54** 1095
Hunt B R, Gallas J A C, Grebogi C, Yorke J A and Koçak H *Preprint*
[6] McDonald S W, Grebogi C, Ott E and Yorke J A 1985 *Physica* **17D** 125
Grebogi C, McDonald S W, Ott E and Yorke J A 1983 *Phys. Lett.* **99A** 415
see also [3, section 5.2]
[7] Farmer J D 1985 *Phys. Rev. Lett.* **55** 351
[8] Grebogi C, McDonald S W, Ott E and Yorke J A 1985 *Phys. Lett.* **110A** 1
[9] Grassberger P, Badii R and Politi A 1988 *J. Stat. Phys.* **51** 135
Morita T, Hata H, Mori H, Horita T and Tomita K 1987 *Prog. Theor. Phys.* **78** 511
see also [3, pp 323–6] and references therein